General Disclaimer

One or more of the Following Statements may affect this Document

- This document has been reproduced from the best copy furnished by the organizational source. It is being released in the interest of making available as much information as possible.

- This document may contain data, which exceeds the sheet parameters. It was furnished in this condition by the organizational source and is the best copy available.

- This document may contain tone-on-tone or color graphs, charts and/or pictures, which have been reproduced in black and white.

- This document is paginated as submitted by the original source.

- Portions of this document are not fully legible due to the historical nature of some of the material. However, it is the best reproduction available from the original submission.

SQT

NASA CR-134817

TECHNICAL REPORT

THE APPLICATION OF "STRAIN RANGE PARTITIONING METHOD" TO TORSIONAL CREEP-FATIGUE INTERACTION

by

S. Y. Zamrik

Department of Engineering Science and Mechanics
The Pennsylvania State University
University Park, Pennsylvania

National Aeronautical Space Administration
Research Grant NGR-39-009-034

October 1, 1975

NASA CR-134817

Technical Report

THE APPLICATION OF "STRAIN RANGE PARTITIONING METHOD" TO TORSIONAL CREEP-FATIGUE INTERACTION

by

S. Y. Zamrik

Department of Engineering Science and Mechanics
The Pennsylvania State University
University Park, Pennsylvania

National Aeronautical Space Administration
Research Grant NGR-39-009-034

October 1, 1975

Table of Contents

List of Illustrations

List of Tables

Nomenclature

$\Delta\varepsilon_{pp}$	Plastic strain in tension and compression
$\Delta\varepsilon_{cc}$	Creep strain in tension and compression
$\Delta\varepsilon_{pc}$	Plastic strain in tension and creep strain in compression
$\Delta\varepsilon_{cp}$	Creep strain in tension and plastic strain in compression
$\Delta\gamma$	Total torsional inelastic shear strain range
$\Delta\gamma_{pp}$	Completely reversed plastic shear strain
$\Delta\gamma_{cc}$	Completely reversed creep shear strain
$\Delta\gamma_{pc}$	Plastic shear strain reversed by creep shear strain
$\Delta\gamma_{cp}$	Creep shear strain reversed by plastic shear strain
N	Observed number of cycles to failure
N_{cp}	Cyclic life associated with a given $\Delta\gamma_{cp}$ strain range
N_{cc}	Cyclic life associated with a given $\Delta\gamma_{cc}$ strain range
N_{pp}	Cyclic life associated with a given $\Delta\gamma_{pp}$ strain range
α, C	Material constants

Abstract

The method of strain range partitioning was applied to a series of torsional fatigue tests conducted on tubular 304 stainless steel specimens at 1200°F (649°C). Creep strain was superimposed on cycling strain, and the resulting strain range was partitioned into four components; completely reversed plastic shear strain, plastic shear strain followed by creep strain, creep strain followed by plastic strain and completely reversed creep strain. Each strain component was related to the cyclic life of the material. The damaging effects of the individual strain components were expressed by a linear life fraction rule. The plastic shear strain component showed the least detrimental factor when compared to creep strain reversed by plastic strain. In the latter case, a reduction of torsional fatigue life in the order of magnitude of 1.5 was observed.

Introduction

In recent years, several approaches have been proposed to treat the effect of creep on fatigue life of metals at elevated temperatures. Methods such as 10% rule [1], the frequency modified life relationship [2], and the characteristic slope relationship [3] have been used in design analysis; however, these types of approaches are limited in use simply because they are based solely on experimental observations rather than on basic mechanisms of deformation which produces a creep-fatigue interaction that influences the material behavior. A promising method that considers mechanisms of deformation was proposed by Manson, Halford and Hirschberg [4] under the name of "strain range partitioning". Although the method is new and has not yet been fully explored, it has given researchers a closer look into the type of deformation a material undergoes as a result of cyclic loading at high temperature and has isolated the types of deformation that may influence fatigue failure.

In this report, the applicability of the strain range partitioning concept in the treatment of torsional creep-fatigue interaction of 304 stainless steel material at 1200°F (649°C) has been examined.

Experimental Details

1. Material and Specimens

The material used in this study was 304 stainless steel extruded in rod form a diameter of one inch (25.4 mm). Specimens were machined and honed according to specifications as shown in Figure (1). Two keyways on each end of the specimen were cut to provide the torsional loading.

HIGH-TEMP. FATIGUE SPECIMEN

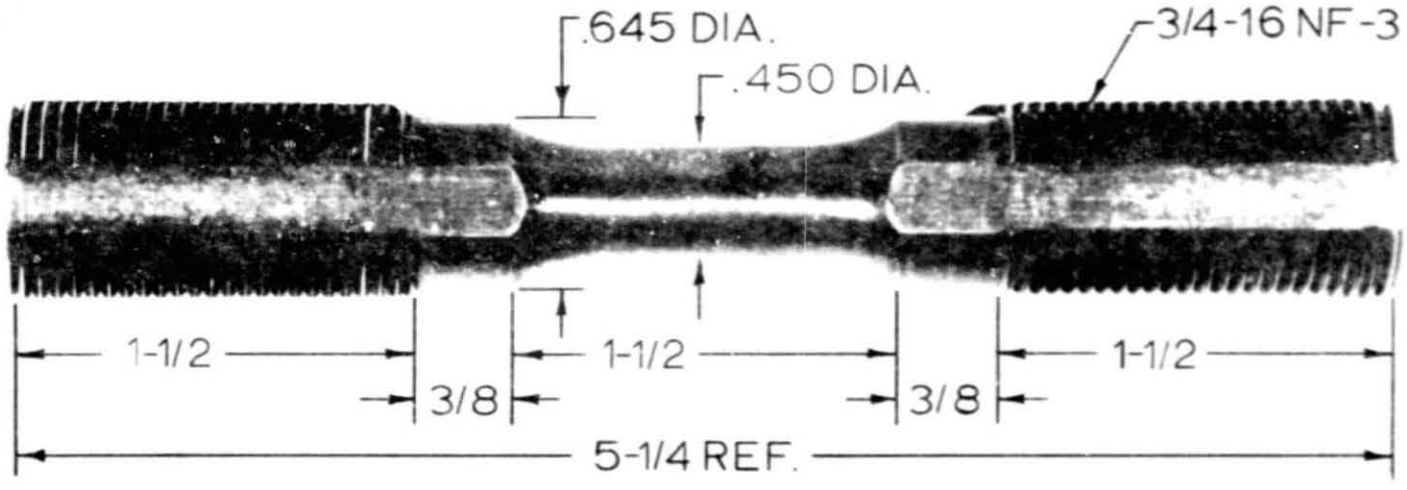

NOTES: GROOVES ARE .250 WIDE X .062 DEEP
FILLET RADIUS IS 3/4
.060 WALL THICKNESS OVER GAGE LENGTH

Figure 1

After machining, specimens were annealed for 30 minutes in an argon environment at 2000°F (1092°C).

The chemical composition and mechanical properties of the material are shown in Tables (1) and (2), respectively.

2. Specimen Heating and Control

The temperature was imposed on specimens through a glo-bar heating element manufactured by the Carborundum Corporation. The element, 6-3/4 inches (171.5 mm) long with 1/4 inch (6.4 mm) diameter, is of silicon carbide with a central heating section or "hot zone" that varies from 1/2 inch (12.7 mm) to 2 inches (80.8 mm) long. The element was inserted in the tubular specimen and left free to expand or contract. Electrical connections were made through aluminum metallized terminals.

The temperature was controlled through two spot welded chromel-alumel thermocouples on the specimen. Signal from these thermocouples was fed to a temperature power controller system that provided power supply.

3. Experimental Equipment

Fatigue tests were carried out on an electro-hydraulic closed loop testing machine specially designed to test thin-walled tubes under combined axial and torsional loading conditions. The axial loading system is completely independent from the torsional system; thus, various ratios between axial and torsional strains can be imposed. These two strains can be applied simultaneously (in-phase) or a time delay can be introduced between them (out-of-phase). The out-of-phase strain capability ranges from 0° to 180°.

Table 1 - Chemical Composition for 304 Stainless Steel

Element	% Weight
Carbon	0.048
Manganese	1.340
Phosphorous	0.039
Silicon	0.500
Chromium	18.600
Nickel	10.100
Cobalt	0.100
Molybdenum	0.300
Columbium	0.002
Copper	0.200
Nitrogen	0.030
Tin	0.018
Lead	0.002
Tantalum	0.002

Table 2 - Mechanical Properties of 304 Stainless Steel

Test Temp. [°F (°C)]	Strain Rate min^{-1}	0.2 % Yield Stress [ksi (MPa)]	Ultimate Strength [ksi (MPa)]	Elongation in 2.375 in (60.3 mm) %	Reduction in Area (a) %	Fracture Ductility (b) %
Room	0.0421	27.4 (189)	78.2 (539)	42.11	75.61	141.10
1200 (649)	0.0421	10.7 (74)	36.8 (254)	16.30	35.68	44.47

(a) Reduction in area: $RA = (A_i - A_f)/A_i$, where A_i is initial area A_f is final area

(b) Fracture ductility: $FD = \ln 1/(1-RA)$

Because of high temperature environment, the axial strain was controlled through an LVDT extensometer and the torsional shear strain through an RVDT extensometer. Both extensometers were calibrated with strain gauges at room temperature.

A major portion of the equipment and test procedure used to generate the data for this investigation were described in detail in reference [5]. Only the new or modified equipment and procedures will be included here. These modifications were necessary only for those tests involving creep shear strain under constant torsional load. In these tests, the load was servo-controlled until a creep shear strain limit was reached. When this strain limit was reached the load was reversed. To prevent load overshoot and to limit the rate of straining to a reasonable level, the oil supplied to the hydraulic rotary actuator was throttled down with a needle valve. Figure (2) and (3) show the new creep cycling unit and its block diagram, respectively.

It should be pointed out that a constant cycling frequency cannot be programmed but has to be dictated by the amount of creep the material exhibits.

Partitioning Inelastic Shear Strain Range

The strain range partitioning concept implies that four distinct inelastic strains exist. These components are the result of mixing plastic flow and creep in one cycle. Therefore, it is possible to partition a cycle into a completely reversed plastic strain, $\Delta\varepsilon_{pp}$, a completely reversed creep strain, $\Delta\varepsilon_{cc}$, a tensile plastic strain followed by compressive

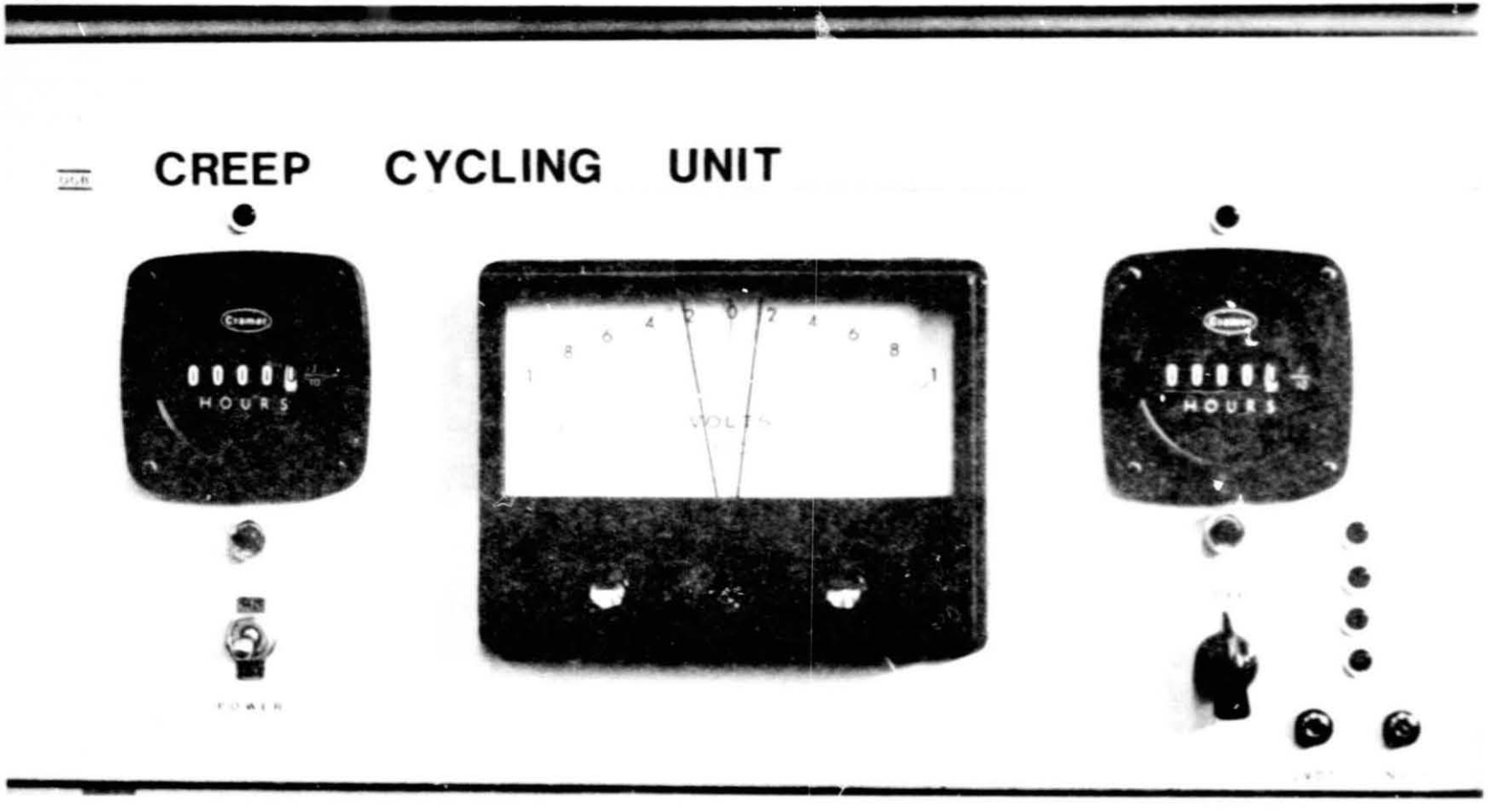

Figure 2 - Creep Cycling Unit

CREEP CYCLING UNIT PART LIST

R - 1000 ohm / 1W Resistor

TL- 110 V neon bulb (Tension)

CL- 110 V neon bulb (Compression)

K - 110 V 4P DT Relay

TS- Toggle Switch DPDT (Tension)

CS- Toggle Switch DPDT (Compression)

MS- Toggle Switch DPDT (Power Switch)

F - Fuse

METER: API Type 5 V DC

Terminal 10 Position

Tension Clock: 4 - 6

Compression Clock: 4 - 10

Total Clock: 4 - 3

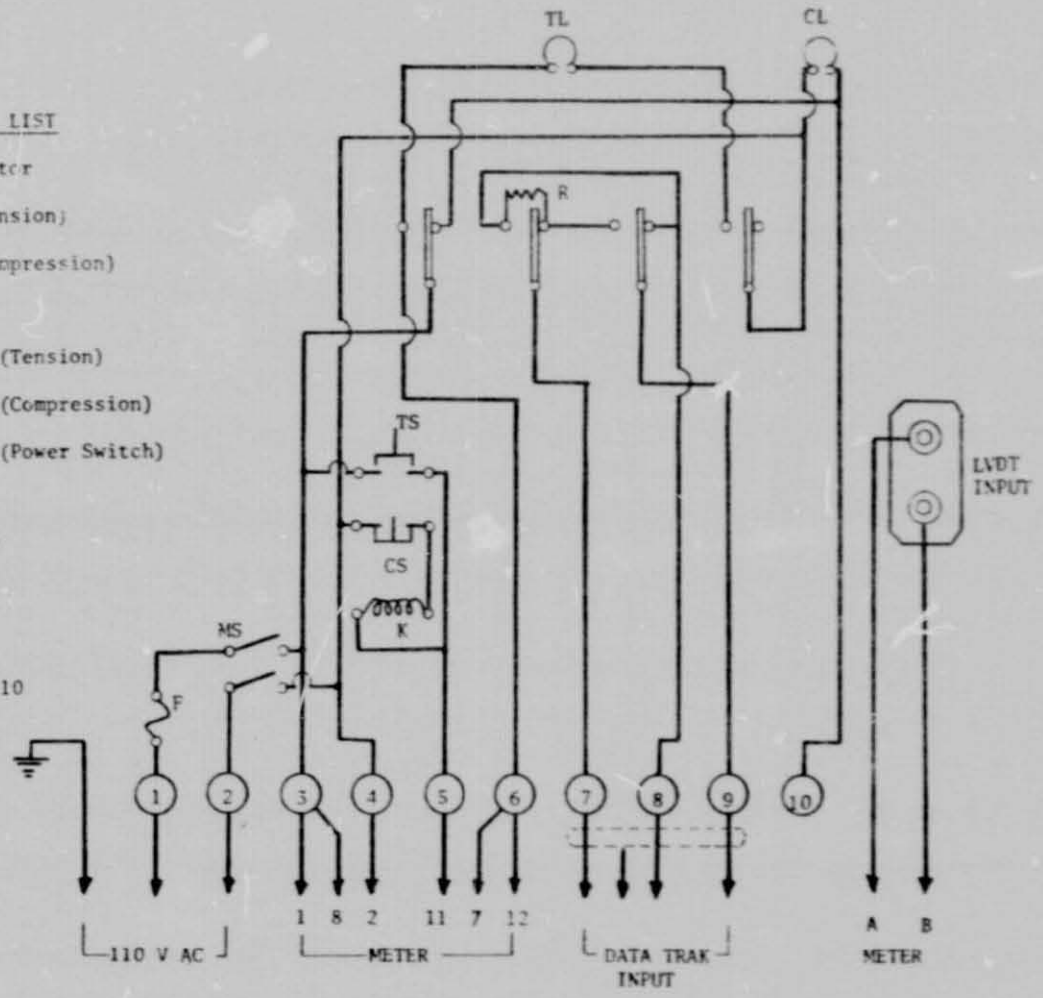

Figure 3 - Block Diagram of Creep Cycling Unit

creep strain, $\Delta\varepsilon_{pc}$, or tensile creep strain followed by compressive plastic strain, $\Delta\varepsilon_{cp}$.

Each type of strain bears a different relation to life. Therefore, it is essential that these individual components be isolated. Once this, is done, each component can be related to the cyclic life of the material through a linear damage summation rule.

In treating torsional creep-fatigue, it is assumed that the total inelastic shear strain in one cycle can also be partitioned into four similar strain components with corresponding cyclic lives. The simplest measurable component is the plastic shear strain $\Delta\gamma_{pp}$ which can be obtained from a completely reversible torsional strain cycling at a rapid loading that will eliminate any induced creep strain. This type of test will result in a hysteresis loop as shown in Figure (4), where cycling is carried between the strain limits A and C. The width of the loop $\overline{BD}$ represents $\Delta\gamma_{pp}$ which can be related to the cyclic life through Manson-Coffin type equation [6] in the form of

$$\Delta\gamma_{pp} \, N_{pp}^{\alpha} = C \tag{1}$$

A straight line fit of $\log(\Delta\gamma_{pp})$ versus $\log(N_{pp})$ establishes the desired relationship.

The other three shear strain components have to be determined from tests specially designed to produce a hysteresis loop which includes creep strain. In axial case, the concept shows a distinction between $\Delta\varepsilon_{cp}$ and $\Delta\varepsilon_{pc}$ components, whereas, in the pure torsion strain cycling case, the cp and pc components are equal; in other words, creep strain

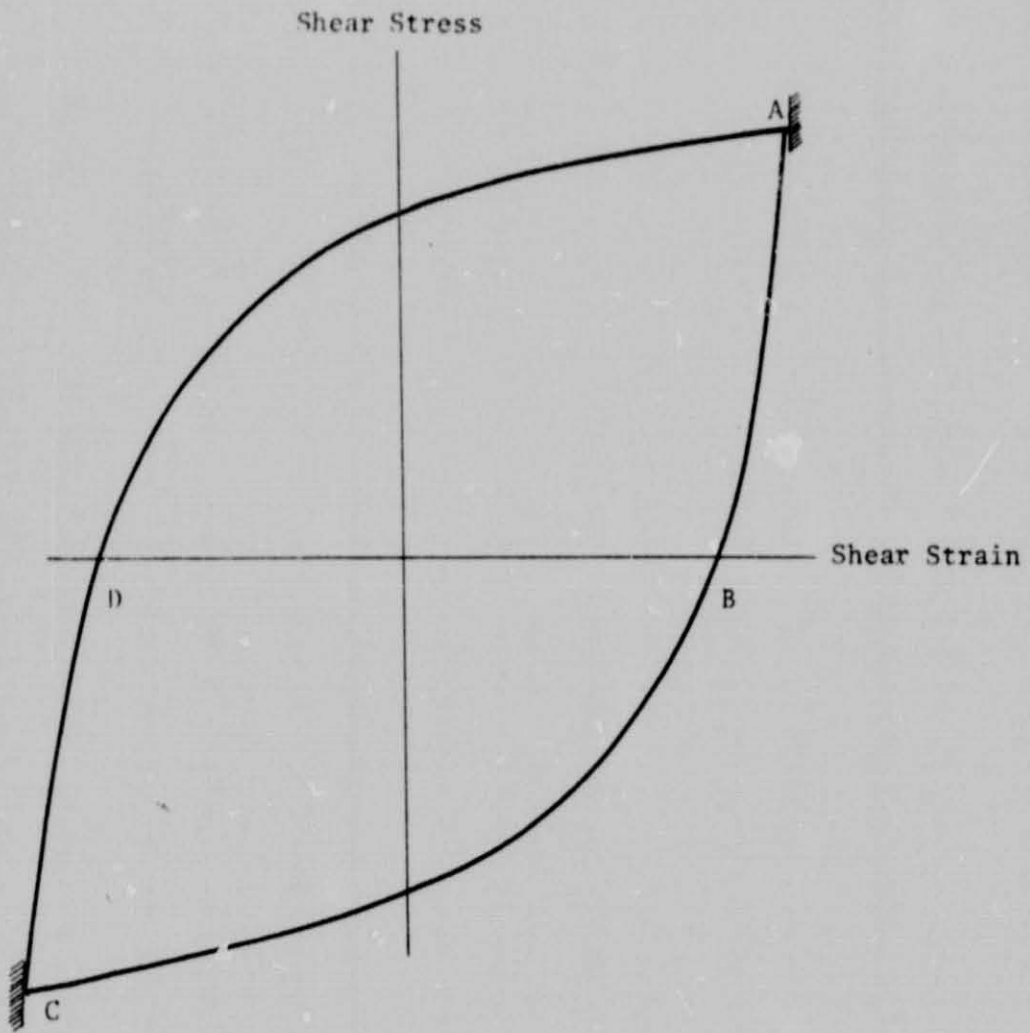

Figure 4 - Hysteresis Loop for a Completely Reversible Plastic Shear Strain Under Torsional Cycling

reversed by plastic shear strain is the same as plastic shear strain reversed by creep shear strain. Distinction is not made between tensile or compressive shear strain since the loading direction is either clockwise or counterclockwise; therefore, in torsional cycling three components of strains exists rather than four.

A hysteresis loop for a cp type shear strain cycling in which a portion of the cycle induces creep shear strain is shown in Figure (5). The loop width represents the total inelastic shear strain was partitioned into $\Delta\gamma_{cp}$ ($\overline{BF}$) and $\Delta\gamma_{pp}$ ($\overline{EF}$). The life that corresponds to the partitioned plastic shear strain $\Delta\gamma_{pp}$ can be found from equation (1); while the remaining life is attributed to the effect of the creep, can be calculated from an assumed linear damage summation in the form of:

$$\frac{N}{N_{pp}} + \frac{N}{N_{cp}} = 1 \qquad (2)$$

where N is the total experimental life determined by a $\Delta\gamma_{cp}$ type test.

The third creep-creep shear strain component $\Delta\gamma_{cc}$ cannot be imposed in an experimental procedure without any plastic component. Therefore, a new type of hysteresis loop has to be generated as shown in Figure (6). The resulting total inelastic shear strain $\overline{EB}$ can then be partitioned into three components: $\Delta\gamma_{pp} = \overline{HB}$, $\Delta\gamma_{cc} = \overline{FB}$ and $\Delta\gamma_{cp} = \Delta\gamma - (\Delta\gamma_{cc} + \Delta\gamma_{pp})$ or $\Delta\gamma_{cp} = \overline{EB} - \overline{FB} - \overline{HB}$. The corresponding life of $\Delta\gamma_{cc}$ is N_{cc} which has to be calculated through the relation:

$$\frac{N}{N_{pp}} + \frac{N}{N_{cp}} + \frac{N}{N_{cc}} = 1 \qquad (3)$$

where N is the total experimental life determined by a $\Delta\gamma_{cc}$ type test.

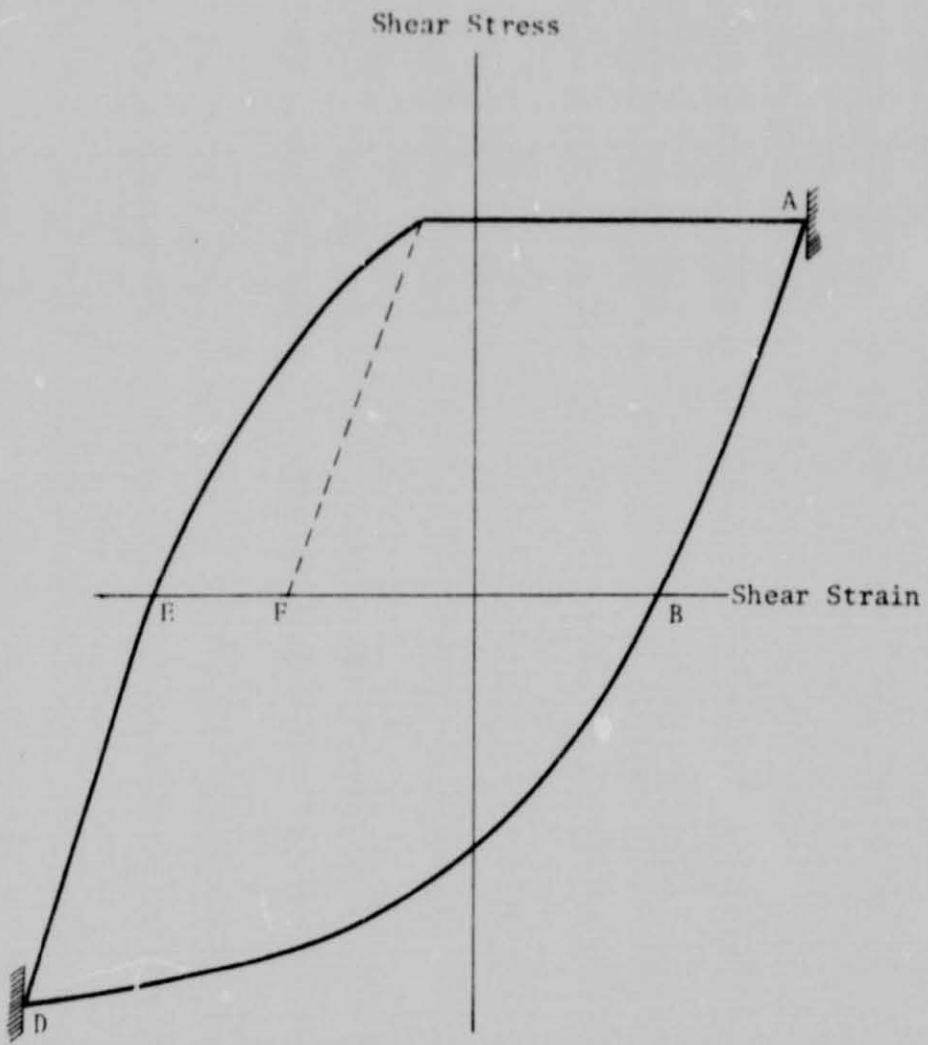

Figure 5 - Hysteresis Loop for $\Delta\gamma_{cp}$ Type Shear Strain Test

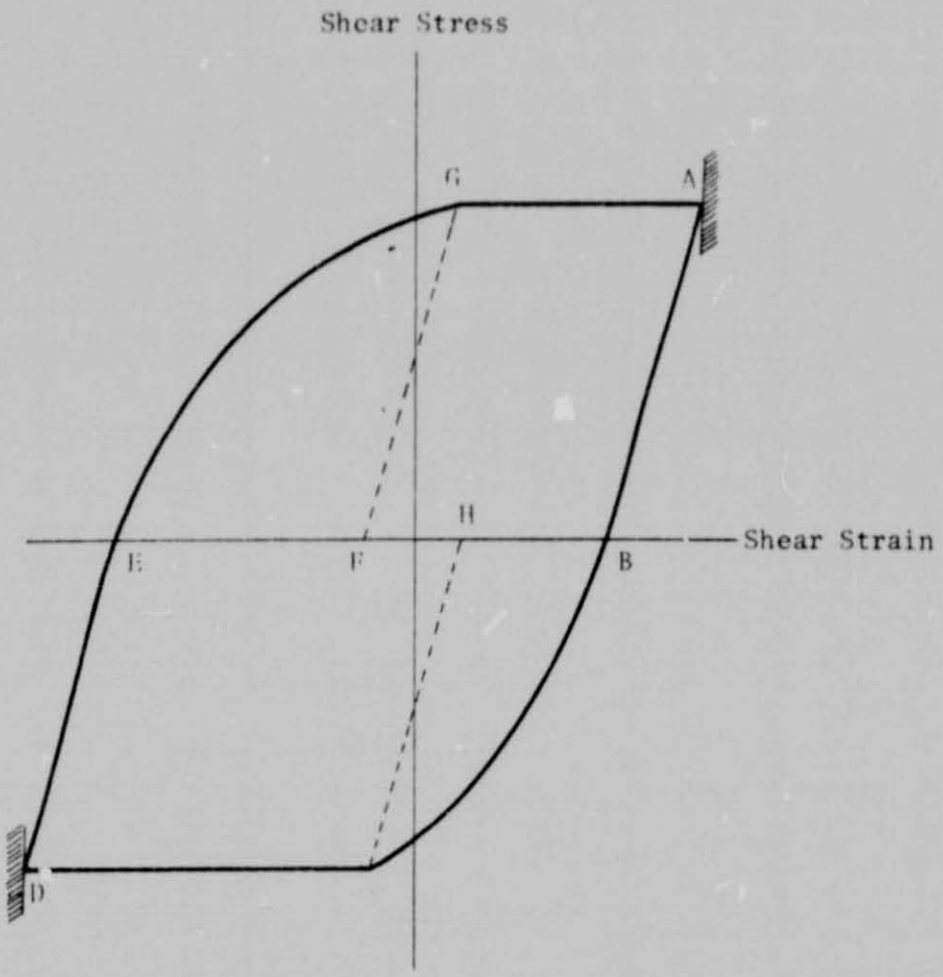

Figure 6 - Hysteresis Loop for $\Delta\gamma_{cc}$ Type Creep Shear Strain Test

Once the individual partitioned shear strain components and their respective lives have been determined, a series of $\Delta\gamma$-N diagrams can be established. Caution must be exercised in determining N_{pp} experimentally, otherwise, error will result in the entire life calculation procedure.

Test Results and Discussion

All shear strain range partitioning tests were performed under pure torsional loading. Figure (7) and (8) show the recorded hysteresis loops obtained under cp and cc type tests.

Limited number of tests were conducted at 1200°F (649°C) to generate the individual inelastic shear strain range versus life relations. The entire test program consisted of 14 tests, 4 tests under a completely reversed torsion that produced $\Delta\gamma_{pp}$, 6 tests under clockwise creep shear strain reversed by plastic shear strain, and the remaining 4 tests were performed under completely reversed creep cycling.

Table (3) summarizes the basic cyclic shear strain-life data obtained on this material. Figure (9) shows the three partitioned shear strain range life relationships. The plastic shear strain range $\Delta\gamma_{pp}$ as measured from the hysteresis loop and the observed number of cycles to failure N_{pp} is shown in Figure (9). These data points were obtained at a frequency of 25 cpm where the creep effect was eliminated. According to the line shown in this figure, a power low relationship was obtained as:

$$\Delta\gamma_{pp} = 2.25\ (N_{pp})^{-0.65} \qquad (4)$$

The relationship between $\Delta\gamma_{cp}$ and life N_{cp} is shown also in Figure (9).

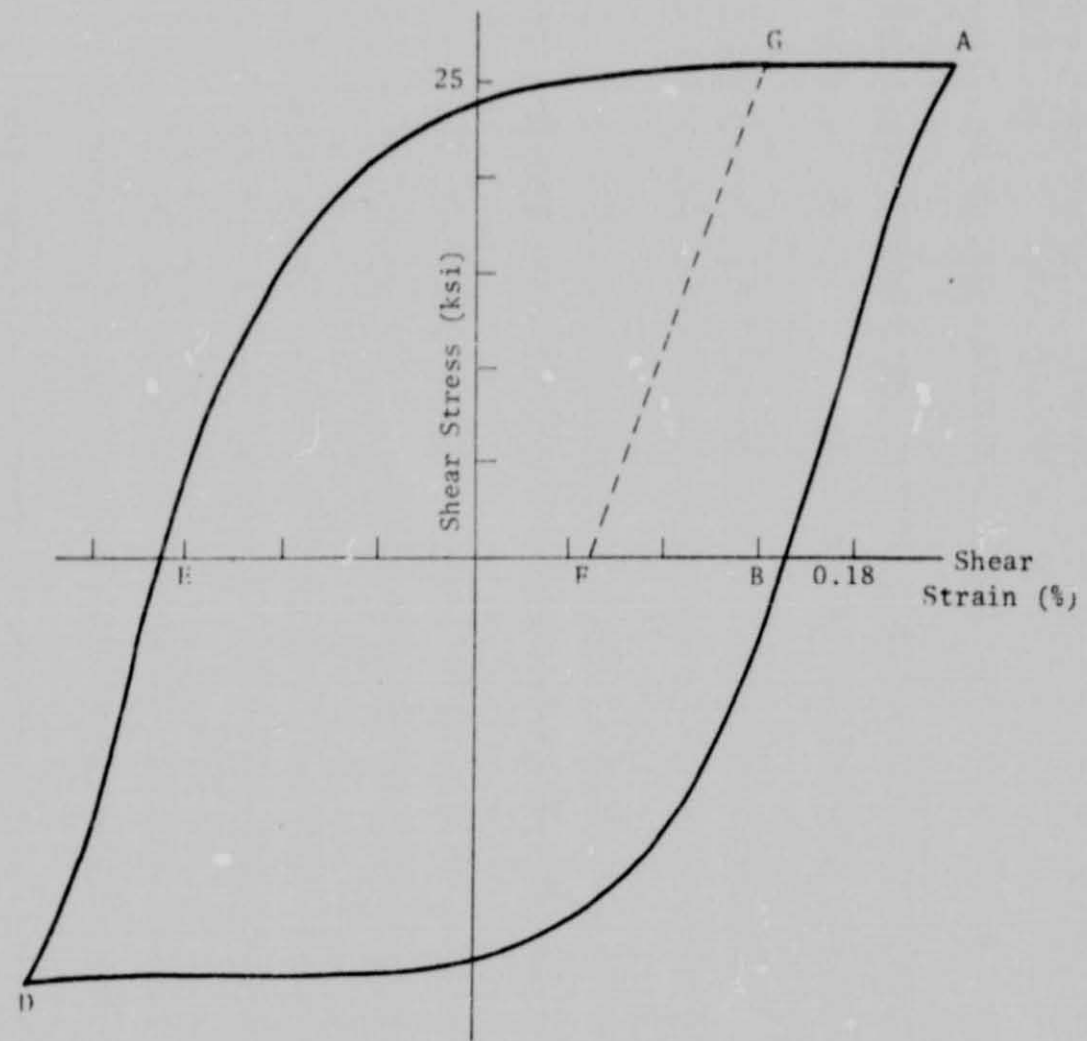

Figure 7 - Recorded Hysteresis Loop Under Torsional $\Delta\gamma_{cp}$ Test - (Test No. 7)

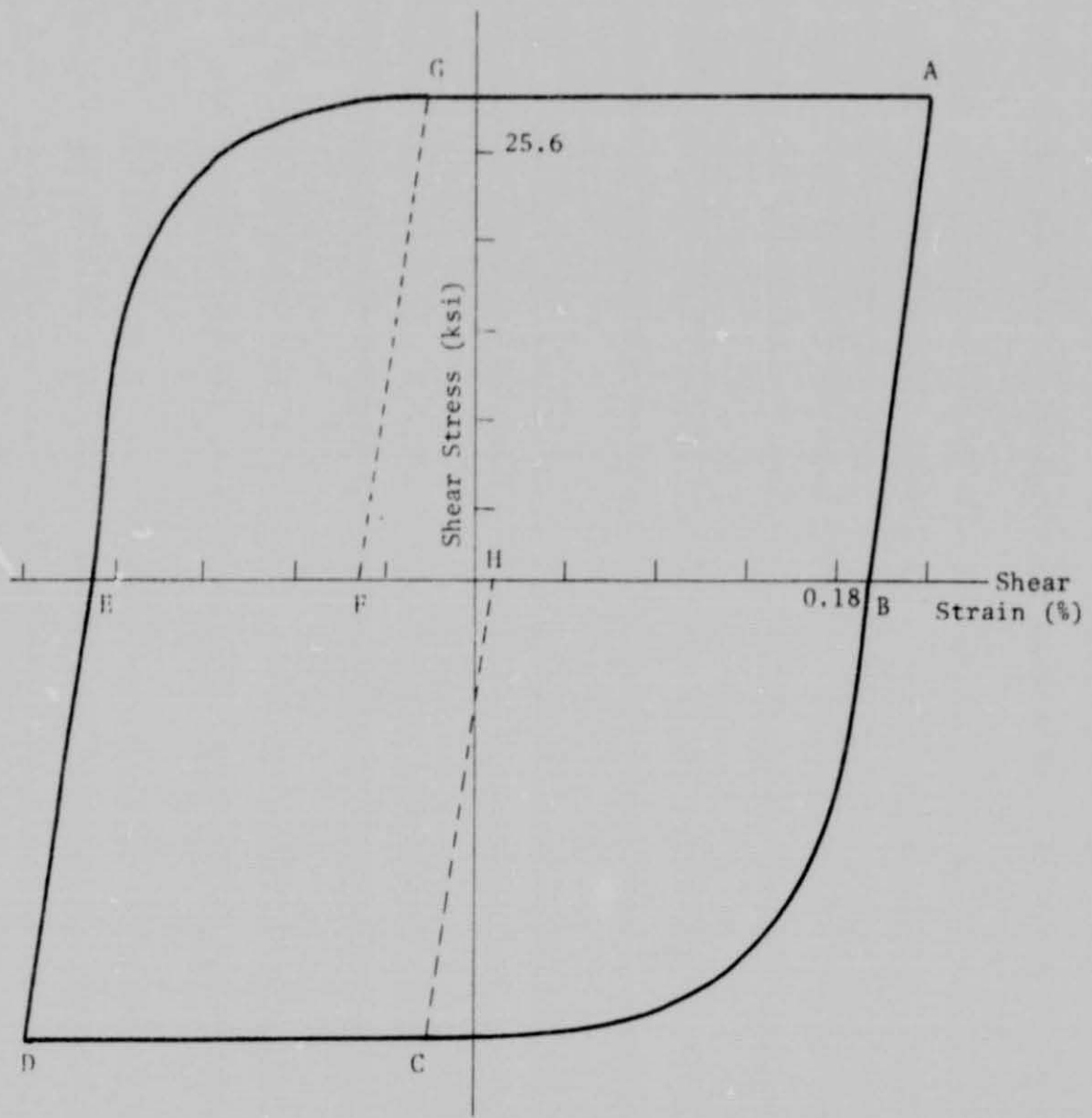

Figure 8 - Recorded Hysteresis Loop Under Torsional $\Delta\gamma_{cc}$ Test - (Test No. 12)

Table 3 - Experimental Test Results Under Torsional Cycling

Test Number	Total Inelastic Shear Strain Range %	Observed # of Cycles N	$\Delta\gamma_{pp}$ %	N_{pp} Cycles	$\Delta\gamma_{cp}$ %	N_{cp} (Calculated) Cycles	$\Delta\gamma_{cc}$ %	N_{cc} (Calculated) Cycles
1	3.52	585	3.520	585	-	-	-	-
2	1.62	2060	1.620	2060	-	-	-	-
3	6.45	230	6.450	230	-	-	-	-
4	0.90	5234	0.900	5234	-	-	-	-
5	2.87	55	1.160	350	1.710	56	-	-
6	2.88	44	0.270	35000	2.610	44	-	-
7	2.88	90	1.970	1500	0.900	96	-	-
8	3.42	114	2.790	880	0.630	131	-	-
9	2.43	148	2.030	1400	0.400	160	-	-
10	2.70	268	2.520	990	0.180	370	-	-
11	1.23	142	0.395	19000	0.315	230	0.520	378
12	3.87	52	1.305	2900	0.630	130	1.935	90
13	2.88	60	0.720	7400	0.990	90	1.170	184
14	1.89	84	0.270	35000	0.360	205	1.260	144

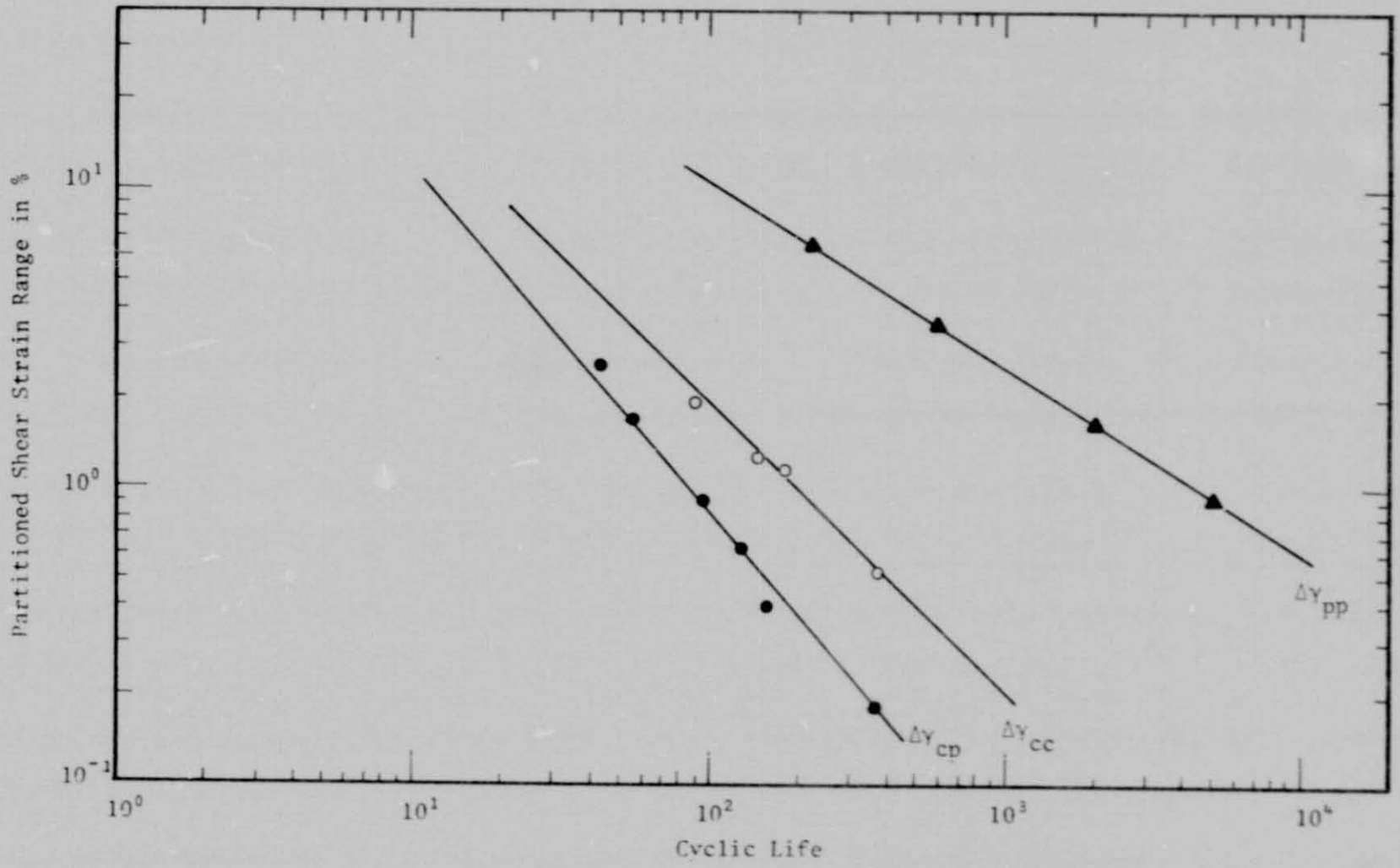

Figure 9 - Partitioned Plastic Shear Strain Range Components Under Torsional Loading

An equation that represents the best fit has the form of:

$$\Delta\gamma_{cp} = 2.40\ (N_{cp})^{-1.22} \tag{5}$$

The cp component has exhibited the most detrimental creep effect on life reduction. This can be seen best when the third shear creep strain component and $\Delta\gamma_{cc}$ is evaluated. The resultant equation representing the relationship between $\Delta\gamma_{cc}$ and life N_{cc} was:

$$\Delta\gamma_{cc} = 1.45\ (N_{cc})^{-0.96} \tag{6}$$

It is difficult to make a proper comparison between the behavior of the material under axial and torsional strain partitioning since axial data is not available at this time; however, a general observation can be made. In the axial case, three partitioned strain components exhibited a common slope characteristic, however, in the torsional case, the material showed different degrees of strain-life slopes characteristics depending on the type of strain that was applied. A possible explanation of this difference may lie in the measure of the ductility, which was difficult to determine in torsion, and perhaps in the amount of hardening that may have occurred in torsional strain, since this material exhibits a strain hardening characteristic. In either case, the $\Delta\gamma_{pp}$ component showed the least detrimental effect on life while the $\Delta\gamma_{cp}$ component showed the most detrimental effect. A characteristic similar to that observed in axial strain partitioning. For the material tested at 1200°F (649°C) a large reduction in life was recorded between these two components. For example, at 1% level a factor of 50 was observed.

Conclusion

The strain range partitioning method has been applied to torsional creep-fatigue analysis. It was found that three strain components exist as compared to four axial components. The torsional cp-component has shown a severe detrimental effect on cyclic life when compared to pp-component, a characteristic that was observed in axial partitioning. The partitioned strain components, whether shear or axial, have shown a similarity in their behavior but with different degrees in slope characteristics when related to a specific number of cycles.

Acknowledgement

The investigator gratefully acknowledges the assistance of Mr. O. G. Bilir in preparing and conducting the tests. These tests were part of his thesis program conducted under the supervision of the author.

References

[1] Manson, S. S., "Interfaces Between Fatigue, Creep and Fracture," International Journal of Fracture Mechanics, Vol. 2, No. 1, March 1966, pp. 327-363.

[2] Coffin, L. F., Jr., "Fatigue at High Temperature," Fatigue at Elevated Temperatures, ASTM STP 520, American Society for Testing and Material, 1973, pp. 5-34.

[3] Berling, J. T. and Conway, J. B., "A New Approach to the Prediction of Low-Cycle Fatigue Data," Metallurgical Transactions, Vol. 1, No. 4, April 1970, pp. 805-809.

[4] Manson, S. S., Halford, G. R., and Hirschberg, M. H., "Creep Fatigue Analysis by Strain-Range Partitioning," Design for Elevated Temperature Environment; American Society of Mechanical Engineers, New York, 1971, pp. 12-28.

[5] Zamrik, S. Y., "The Effects of Out-of-Phase, Biaxial Strain Cycling on Low-Cycle Fatigue," NASA CR-72843 Technical Report, January 1972.

[6] Manson, S. S., "Behavior of Metals under Conditions of Thermal Stress," NACA TN 2933, 1953.

[7] Manson, S. S., "The Challenge to Unify Treatment of High Temperature Fatigue - Partisan Proposal Based on Strain Range Partitioning," Fatigue at Elevated Temperatures, ASTM STP 520, American Society for Testing and Materials, 1973, pp. 744-782.